Tellus SERIES A DYNAMIC METEOROLOGY AND OCEANOGRAPHY
PUBLISHED BY THE INTERNATIONAL METEOROLOGICAL INSTITUTE IN STOCKHOLM

Tellus (2009), 61A, 428–437
Printed in Singapore. All rights reserved

© *2009 The Authors*
Journal compilation © *2009 Blackwell Munksgaard*
TELLUS

Comparison of retrospective optimal interpolation with four-dimensional variational assimilation

By HYO-JONG SONG[1], GYU-HO LIM[1*], DONG-IN LEE[2] and HEE-SANG LEE[3], [1]*School of Earth and Environmental Sciences, Seoul National University, Seoul 151-747, Republic of Korea;* [2]*Department of Environmental Atmospheric Sciences, Pukyong National University, Busan 606-739, Republic of Korea;* [3]*Forecast Research Laboratory, National Institute of Meteorological Research, Seoul 156-720, Republic of Korea*

(Manuscript received 4 February 2008; in final form 23 January 2009)

ABSTRACT

We propose a retrospective optimal interpolation (ROI) system that is derived from the quasi-static variational assimilation (QSVA) algorithm. Even when the four-dimensional variational assimilation (4D-Var) may fail to find the global minimum of a cost function because the function has multiple minima, ROI is shown to find this minimum. However, ROI's ability to overcome the multiple minima problem depends on the observation time interval over the analysis window. Using the perturbation method, we can implement ROI without using an adjoint model, which is required by QSVA. For cost-effective implementation, we developed a reduced-rank formulation of ROI, based on the accuracy-saturation property.

From numerical experiments using the Lorenz three-variable model, we show that ROI finds the global minimum of the cost function even when the 4D-Var analysis is trapped in a local minimum. From experiments with the Lorenz 40-variable model, we confirm that the reduced-rank formulation becomes demonstrably cost-effective as the analysis window expands. Finally, we demonstrate a possible loss of efficiency of ROI with implications for future research.

1. Introduction

Obtaining high-quality analysis data for a homogeneous field is necessary for understanding the dynamic and physical features of the atmosphere and for forecasting future atmospheric fields (Le Dimet and Talagrand, 1986). We can obtain such high-quality analysis data by using future observations as well as current and past observations. The term retrospective analysis denotes the use of future observations for high-quality analysis (Cohn et al., 1994). As emphasized by Horel and Colman (2005), retrospective analysis is important not only for verifying experimental gridded forecasts but also for producing a climate database that could be used to assess the regional impacts of climate change.

Four-dimensional variational assimilation (4D-Var) is a well-known retrospective analysis method, which has been applied to atmospheric phenomena of various scales (Lorenc, 2003; Ruggiero et al., 2006). For example, Gérard and Saunders (1999) assimilated the total column of the amount of water vapour retrieved from the Special Sensor Microwave Imager to show the impacts of the 4D-Var on the humidity fields in the tropics and Southern Hemisphere and on the meridional circulation. Sun (2005) assimilated single-Doppler observations into a cloud-scale numerical model using 4D-Var to reveal the major structure of a storm.

In 4D-Var, the best analysis is defined as one that minimizes a cost function. Over a given time interval, the 4D-Var analysis at the end of the analysis window is equivalent to a Kalman filter analysis at the same time under the assumptions: the observation operator and the model are linear, model error is neglected and the same background error covariance is used (Lorenc, 1986). 4D-Var, however, is more widely used than the Kalman filter, primarily because the former is computationally more feasible (Rabier et al., 1998).

4D-Var assumes that a zero-gradient solution is the same as the minimizer and produces an analysis by successive correction along the cost function gradients (Le Dimet and Talagrand, 1986). Strong non-linearity in model dynamics may create multiple minima in the cost function (Rabier and Courtier, 1992; Miller et al., 1994). Rabier and Courtier (1992) showed that in strongly baroclinic conditions, multiple minima may appear when the analysis window is too wide to accept the tangent

*Corresponding author.
e-mail: gyuholim@snu.ac.kr
DOI: 10.1111/j.1600-0870.2009.00396.x

linear approximation, in which case, the minimization process may stop after identifying a local minimizer near the initial state of the process (Pires et al., 1996).

The implementation of 4D-Var requires an adjoint model, expressed as the transpose of the tangent linear model. The inclusion of physics schemes into tangent linear models is necessary for assimilating most physical observations (Janiskova et al., 1999). However, the linearization of the numerical formulation of a non-linear model may generate unwanted numerical instabilities, even when the original non-linear formulation guarantees numerical stability and contains no mathematical discontinuities (Errico, 2003). In that case, the linear model generated directly from a non-linear model should be modified, since the adjoint model will then also be influenced by the noise arising from the numerical instability of the tangent linear model. The resulting tangent linear and adjoint models would then be inconsistent with the original model (Zhu and Kamachi, 2000).

To overcome the multiple minima problems associated with model non-linearity, Pires et al. (1996) propose a quasi-static variational assimilation (QSVA) algorithm, but the method still requires an adjoint model. To reduce analysis error due to the multiple minima problem, without using an adjoint model, here we proposed a retrospective optimal interpolation (ROI) algorithm. We detail the derivation of ROI from QSVA and address its accuracy in comparison with that of 4D-Var in Section 2. In Section 3, we describe a reduced-rank formulation of ROI, which results in analysis errors below a designated error tolerance. Using the Lorenz three-variable and the Lorenz 40-variable models, we compare the functionality and efficiency of ROI with that of 4D-Var. In Section 4, we examine the extent to which the ROI analysis is influenced by the analysis window and error tolerance.

2. Comparison of the retrospective optimal interpolation (ROI) with 4D-Var

2.1. *Quasi-static variational assimilation (QSVA)*

Suppose that a state of the atmosphere is represented by $\mathbf{x}_0^{\mathrm{t}}$ and consists of m atmospheric variables at time t_0. The background state $\mathbf{x}_0^{\mathrm{b}}$ is defined as a guess of $\mathbf{x}_0^{\mathrm{t}}$, which is normally distributed around $\mathbf{x}_0^{\mathrm{t}}$ with an $m \times m$ error covariance matrix $\mathbf{B}$. In this formulation, the superscripts t and b of $\mathbf{x}$ denote true and background states, respectively, and the subscript 0 denotes time for t_0. The 4D-Var cost function is conventionally defined as

$$J_N(\mathbf{x}_{\mathrm{o}}) \equiv \frac{1}{2}\left[\mathbf{x}_{\mathrm{o}} - \mathbf{x}_{\mathrm{o}}^{b}\right]^{\mathrm{T}} \mathbf{B}^{-1} \left[\mathbf{x}_{\mathrm{o}} - \mathbf{x}_{\mathrm{o}}^{\mathrm{b}}\right] + \frac{1}{2}\sum_{n=\mathrm{o}}^{N}\left[\mathbf{y}_n^{\mathrm{obs}} - H_n(M_n(\mathbf{x}_{\mathrm{o}}))\right]^{\mathrm{T}} \mathbf{R}_n^{-1}\left[\mathbf{y}_n^{\mathrm{obs}} - H_n(M_n(\mathbf{x}_{\mathrm{o}}))\right], \tag{1}$$

where $\mathbf{y}_0^{\mathrm{obs}}$, $\mathbf{y}_1^{\mathrm{obs}}$, ... and $\mathbf{y}_N^{\mathrm{obs}}$ are serially uncorrelated observation sets at times t_0, t_1, ... and t_N, respectively. We define the analysis window as the length of time covering all observation times and consisting of several observation time intervals. The observations are assumed to be normally distributed about the truth with the corresponding observation error covariance matrices, $\mathbf{R}_0, \mathbf{R}_1, \ldots \mathbf{R}_N$. A forecast model $M_n(\mathbf{x}_0)$ evolves $\mathbf{x}_0$ into the future state $\mathbf{x}_n$ at time t_n, and $M_0(\mathbf{x}_0)$ is equivalent to $\mathbf{x}_0$, which means that the function $M_0(\mathbf{x})$ is an identity. The observation operator $H_n(\mathbf{x}_n)$ transforms the model state $\mathbf{x}_n$ into a state vector in the observation space. The cost function (1) is a measure of the distance to the background state $\mathbf{x}_0^{\mathrm{b}}$ and the N observation data sets contained in the analysis window.

As the analysis window is lengthened in a non-linear dynamical system, the cost function (1) may have multiple minima and hence errors in 4D-Var analysis may increase (Rabier and Courtier, 1992; Miller et al., 1994). To offset this increase of errors, researchers can use the QSVA algorithm proposed by Pires et al. (1996). The QSVA has been shown, with a three-layer quasi-geostrophic model, to converge to the global minimum of the cost function when the analysis window equals 4 d, which is long enough to create multiple minima (Swanson et al., 1998).

In QSVA, the analysis window is progressively increased to a maximum width (Pires et al., 1996). Initially, the analysis window is set to zero, and the cost function $J_0(\mathbf{x}_0)$ is written as

$$J_0(\mathbf{x}_0) = \frac{1}{2}\left[\mathbf{x}_0 - \mathbf{x}_0^{\mathrm{b}}\right]^{\mathrm{T}} \mathbf{B}^{-1}\left[\mathbf{x}_0 - \mathbf{x}_0^{\mathrm{b}}\right] + \frac{1}{2}\left[\mathbf{y}_0^{\mathrm{obs}} - H_0(\mathbf{x}_0)\right]^{\mathrm{T}} \mathbf{R}_0^{-1}\left[\mathbf{y}_0^{\mathrm{obs}} - H_0\left(\mathbf{x}_0\right)\right]. \tag{2}$$

The minimizer of (2) is found by a minimization process, starting with the background state $\mathbf{x}_0^{\mathrm{b}}$. When the analysis window is extended from t_0 to t_1, the cost function $J_1(\mathbf{x}_0)$ is written as

$$J_1(\mathbf{x}_0) = \frac{1}{2}\left[\mathbf{x}_0 - \mathbf{x}_0^{\mathrm{b}}\right]^{\mathrm{T}} \mathbf{B}^{-1}\left[\mathbf{x}_0 - \mathbf{x}_0^{\mathrm{b}}\right] + \frac{1}{2}\left[\mathbf{y}_0^{\mathrm{obs}} - H_0(\mathbf{x}_0)\right]^{\mathrm{T}} \mathbf{R}_0^{-1}\left[\mathbf{y}_0^{\mathrm{obs}} - H_0(\mathbf{x}_0)\right] + \frac{1}{2}\left[\mathbf{y}_1^{\mathrm{obs}} - H_1(M_1(\mathbf{x}_0))\right]^{\mathrm{T}} \mathbf{R}_1^{-1}\left[\mathbf{y}_1^{\mathrm{obs}} - H_1(M_1(\mathbf{x}_0))\right]. \tag{3}$$

Using the minimizer of (2), which is better than $\mathbf{x}_0^{\mathrm{b}}$, as the starting point, the minimizer of (3) can be found. When the analysis window is extended from t_0 to t_n, we formulate the cost function as follows:

$$J_n(\mathbf{x}_0) = \frac{1}{2}\left[\mathbf{x}_0 - \mathbf{x}_0^{\mathrm{b}}\right]^{\mathrm{T}} \mathbf{B}^{-1}\left[\mathbf{x}_0 - \mathbf{x}_0^{\mathrm{b}}\right] + \frac{1}{2}\sum_{i=0}^{n}\left[\mathbf{y}_i^{\mathrm{obs}} - H_i(M_i(\mathbf{x}_0))\right]^{\mathrm{T}} \mathbf{R}_i^{-1}\left[\mathbf{y}_i^{\mathrm{obs}} - H_i(M_i(\mathbf{x}_0))\right], \tag{4}$$

where $n = 0, 1, \ldots$ and N. By recursively minimizing the cost function J_n with the minimizer of the previous cost function J_{n-1} as the starting state, QSVA finds the global minimizer of (1). To minimize $J_1, J_2, \ldots J_N$, QSVA uses the adjoint method; hence it requires an adjoint model.

2.2. Derivation of ROI from QSVA

Assuming that the minimizer of the nth cost function is close enough to the minimizer of the next cost function to guarantee the validity of the tangent linear approximation, we can derive a variant form of QSVA based on an optimal interpolation (OI) formulation. Using the tangent linear approximation with a background state $\mathbf{x}_0^{\mathrm{b}}$ allows us to write the eq. (2) as

$$\begin{aligned} J_0(\mathbf{x}_0) = & \frac{1}{2}\left[\mathbf{x}_0 - \mathbf{x}_0^{\mathrm{b}}\right]^{\mathrm{T}} \mathbf{B}^{-1}\left[\mathbf{x}_0 - \mathbf{x}_0^{\mathrm{b}}\right] \\ & + \frac{1}{2}\left[\mathbf{y}_0^{\mathrm{obs}} - H_0\left(\mathbf{x}_0^{\mathrm{b}}\right) - \mathbf{H}_0\left[\mathbf{x}_0 - \mathbf{x}_0^{\mathrm{b}}\right]\right]^{\mathrm{T}} \\ & \times \mathbf{R}_0^{-1}\left[\mathbf{y}_0^{\mathrm{obs}} - H_0\left(\mathbf{x}_0^{\mathrm{b}}\right) - \mathbf{H}_0\left[\mathbf{x}_0 - \mathbf{x}_0^{\mathrm{b}}\right]\right], \end{aligned} \quad (5)$$

where $\mathbf{H}_0$ is the first-order derivative of $H_0(\mathbf{x})$ with respect to $\mathbf{x}$. Because (5) is quadratic, the zero-gradient solution, which is the solution of the following equation,

$$\begin{aligned} \nabla J_0\left(\mathbf{x}_0\right) = & \mathbf{B}^{-1}\left[\mathbf{x}_0 - \mathbf{x}_0^{\mathrm{b}}\right] - \mathbf{H}_0^{\mathrm{T}} \\ & \times \mathbf{R}_0^{-1}\left[\mathbf{y}_0^{\mathrm{obs}} - H_0\left(\mathbf{x}_0^{\mathrm{b}}\right) - \mathbf{H}_0\left[\mathbf{x}_0 - \mathbf{x}_0^{\mathrm{b}}\right]\right] = 0, \end{aligned} \quad (6)$$

minimizes (5). By manipulating the above equation, we obtain the zero-gradient solution $\mathbf{x}_{(1)}^{\mathrm{a}}$:

$$\mathbf{x}_{(1)}^{\mathrm{a}} = \mathbf{x}_0^{\mathrm{b}} + \left[\mathbf{B}^{-1} + \mathbf{H}_0^{\mathrm{T}}\mathbf{R}_0^{-1}\mathbf{H}_0\right]^{-1}\mathbf{H}_0^{\mathrm{T}}\mathbf{R}_0^{-1}\left[\mathbf{y}_0^{\mathrm{obs}} - H_0\left(\mathbf{x}_0^{\mathrm{b}}\right)\right], \quad (7)$$

in which the parenthesized subscript denotes the number of sequential analyses. The analysis state $\mathbf{x}_{(1)}^{\mathrm{a}}$ is the minimizer of (2) and is equal to the OI analysis if the background state and observation set follow a Gaussian distribution (Kalnay, 2003). The analysis error covariance $\mathbf{P}_{(1)}^{\mathrm{a}}$ is written as

$$\mathbf{P}_{(1)}^{\mathrm{a}} = \left[\mathbf{B}^{-1} + \mathbf{H}_0^{\mathrm{T}}\mathbf{R}_0^{-1}\mathbf{H}_0\right]^{-1}, \quad (8)$$

as shown in Appendix A.

The previous analysis $\mathbf{x}_{(1)}^{\mathrm{a}}$ becomes closer to the minimizer of the cost function (3) than the background state. Then the tangent linear approximation $H_0(\mathbf{x}_{(1)}^{\mathrm{a}}) \approx H_0(\mathbf{x}_0^{\mathrm{b}}) + \mathbf{H}_0[\mathbf{x}_{(1)}^{\mathrm{a}} - \mathbf{x}_0^{\mathrm{b}}]$ can be justified. In terms of the analysis $\mathbf{x}_{(1)}^{\mathrm{a}}$, we write the gradient of the cost function (3) as follows:

$$\begin{aligned} & \nabla J_1(\mathbf{x}_0) = \mathbf{B}^{-1}\left[\mathbf{x}_0 - \mathbf{x}_0^{\mathrm{b}}\right] - \mathbf{H}_0^{\mathrm{T}}\mathbf{R}_0^{-1}\left[\mathbf{y}_0^{\mathrm{obs}} - H_0\left(\mathbf{x}_{(1)}^{\mathrm{a}}\right)\right. \\ & \quad \left.-\mathbf{H}_0\left[\mathbf{x}_0 - \mathbf{x}_{(1)}^{\mathrm{a}}\right]\right] - \mathbf{M}_1^{\mathrm{T}}\mathbf{H}_1^{\mathrm{T}}\mathbf{R}_1^{-1}\left[\mathbf{y}_1^{\mathrm{obs}}\right. \\ & \quad \left.-H_1\left(M_1\left(\mathbf{x}_{(1)}^{\mathrm{a}}\right)\right) - \mathbf{H}_1\mathbf{M}_1\left[\mathbf{x}_0 - \mathbf{x}_{(1)}^{\mathrm{a}}\right]\right] = 0, \\ & \mathbf{B}^{-1}\left[\mathbf{x}_0 - \mathbf{x}_0^{\mathrm{b}}\right] - \mathbf{H}_0^{\mathrm{T}}\mathbf{R}_0^{-1}\left[\mathbf{y}_0^{\mathrm{obs}} - H_0\left(\mathbf{x}_0^{\mathrm{b}}\right) - \mathbf{H}_0\left[\mathbf{x}_{(1)}^{\mathrm{a}} - \mathbf{x}_0^{\mathrm{b}}\right]\right. \\ & \quad \left.-\mathbf{H}_0\left[\mathbf{x}_0 - \mathbf{x}_{(1)}^{\mathrm{a}}\right]\right] - \mathbf{M}_1^{\mathrm{T}}\mathbf{H}_1^{\mathrm{T}}\mathbf{R}_1^{-1}\left[\mathbf{y}_1^{\mathrm{obs}} - H_1\left(M_1\left(\mathbf{x}_{(1)}^{\mathrm{a}}\right)\right)\right. \\ & \quad \left.-\mathbf{H}_1\mathbf{M}_1\left[\mathbf{x}_0 - \mathbf{x}_{(1)}^{\mathrm{a}}\right]\right] = 0, \\ & \mathbf{B}^{-1}\left[\mathbf{x}_0 - \mathbf{x}_0^{\mathrm{b}}\right] + \mathbf{H}_0^{\mathrm{T}}\mathbf{R}_0^{-1}\mathbf{H}_0\left[\mathbf{x}_0 - \mathbf{x}_{(1)}^{\mathrm{a}}\right] \\ & \quad -\mathbf{H}_0^{\mathrm{T}}\mathbf{R}_0^{-1}\left[\mathbf{y}_0^{\mathrm{obs}} - H_0\left(\mathbf{x}_0^{\mathrm{b}}\right)\right] + \mathbf{H}_0^{\mathrm{T}}\mathbf{R}_0^{-1}\mathbf{H}_0\left[\mathbf{x}_{(1)}^{\mathrm{a}} - \mathbf{x}_0^{\mathrm{b}}\right] \\ & \quad -\mathbf{M}_1^{\mathrm{T}}\mathbf{H}_1^{\mathrm{T}}\mathbf{R}_1^{-1}\left[\mathbf{y}_1^{\mathrm{obs}} - H_1\left(M_1\left(\mathbf{x}_{(1)}^{\mathrm{a}}\right)\right) - \mathbf{H}_1\mathbf{M}_1\left[\mathbf{x}_0 - \mathbf{x}_{(1)}^{\mathrm{a}}\right]\right] = 0, \\ & \left[\mathbf{B}^{-1} + \mathbf{H}_0^{\mathrm{T}}\mathbf{R}_0^{-1}\mathbf{H}_0\right]\left[\mathbf{x}_0 - \mathbf{x}_0^{\mathrm{b}}\right] - \left[\mathbf{B}^{-1} + \mathbf{H}_0^{\mathrm{T}}\mathbf{R}_0^{-1}\mathbf{H}_0\right]\left[\mathbf{x}_{(1)}^{\mathrm{a}} - \mathbf{x}_0^{\mathrm{b}}\right] \\ & \quad -\mathbf{M}_1^{\mathrm{T}}\mathbf{H}_1^{\mathrm{T}}\mathbf{R}_1^{-1}\left[\mathbf{y}_1^{\mathrm{obs}} - H_1\left(M_1\left(\mathbf{x}_{(1)}^{\mathrm{a}}\right)\right) - \mathbf{H}_1\mathbf{M}_1\left[\mathbf{x}_0 - \mathbf{x}_{(1)}^{\mathrm{a}}\right]\right] = 0, \end{aligned} \quad (9)$$

where $\mathbf{M}_1$ is the first derivative of $M_1(\mathbf{x})$ with respect to $\mathbf{x}$. Here, we use the equality, $\mathbf{H}_0^{\mathrm{T}}\mathbf{R}_0^{-1}[\mathbf{y}_0^{\mathrm{obs}} - H_0(\mathbf{x}_0^{\mathrm{b}})] = [\mathbf{B}^{-1} + \mathbf{H}_0^{\mathrm{T}}\mathbf{R}_0^{-1}\mathbf{H}_0][\mathbf{x}_{(1)}^{\mathrm{a}} - \mathbf{x}_0^{\mathrm{b}}]$ by referring to the eq. (7). The solution of the eq. (9) is

$$\begin{aligned} \mathbf{x}_{(2)}^{\mathrm{a}} = & \mathbf{x}_{(1)}^{\mathrm{a}} + \left[\mathbf{P}_{(1)}^{\mathrm{a}} + \mathbf{M}_1^{\mathrm{T}}\mathbf{H}_1^{\mathrm{T}}\mathbf{R}_1^{-1}\mathbf{H}_1\mathbf{M}_1\right]^{-1} \\ & \times \mathbf{M}_1^{\mathrm{T}}\mathbf{H}_1^{\mathrm{T}}\mathbf{R}_1^{-1}\left[\mathbf{y}_1^{\mathrm{obs}} - H_1\left(M_1\left(\mathbf{x}_{(1)}^{\mathrm{a}}\right)\right)\right]. \end{aligned} \quad (10)$$

This equation represents a new kind of OI formulation, which, in contrast to conventional OI, retrospectively assimilates an observation set $\mathbf{y}_1^{\mathrm{obs}}$ at a future time t_1 into the analysis $\mathbf{x}_{(1)}^{\mathrm{a}}$ at time t_0. By referring to the derivation of $\mathbf{P}_{(1)}^{\mathrm{a}}$, we can obtain the corresponding error covariance $\mathbf{P}_{(2)}^{\mathrm{a}}$,

$$\mathbf{P}_{(2)}^{\mathrm{a}} = \left[\mathbf{P}_{(1)}^{\mathrm{a}} + \mathbf{M}_1^{\mathrm{T}}\mathbf{H}_1^{\mathrm{T}}\mathbf{R}_1^{-1}\mathbf{H}_1\mathbf{M}_1\right]^{-1}. \quad (11)$$

When the prior analysis $\mathbf{x}_{(n)}^{\mathrm{a}}$ is used as the state vector on which the next cost function J_n is linearized, the gradient of the cost function (4) is

$$\begin{aligned} \nabla J_n(\mathbf{x}_0) = & \mathbf{B}^{-1}\left[\mathbf{x}_0 - \mathbf{x}_0^{\mathrm{b}}\right] - \sum_{i=0}^{n}\mathbf{M}_i^{\mathrm{T}}\mathbf{H}_i^{\mathrm{T}}\mathbf{R}_i^{-1} \\ & \times\left[\mathbf{y}_i^{\mathrm{obs}} - H_i\left(M_i\left(\mathbf{x}_{(n)}^{\mathrm{a}}\right)\right) - \mathbf{H}_i\mathbf{M}_i\left[\mathbf{x}_0 - \mathbf{x}_{(n)}^{\mathrm{a}}\right]\right] = 0. \end{aligned} \quad (12)$$

Because $\mathbf{x}_{(i)}^{\mathrm{a}}$ approaches $\mathbf{x}_{(n)}^{\mathrm{a}}$, even though the model non-linearity becomes stronger, as i increases, we may assume the following relationship:

$$\begin{aligned} & H_i\left(M_i\left(\mathbf{x}_{(n)}^{\mathrm{a}}\right)\right) \approx H_i\left(M_i\left(\mathbf{x}_{(i)}^{\mathrm{a}}\right)\right) \\ & \quad + \mathbf{H}_i\mathbf{M}_i\left[\mathbf{x}_{(n)}^{\mathrm{a}} - \mathbf{x}_{(i)}^{\mathrm{a}}\right] \quad \text{for} \quad i = 0, \ldots, n, \end{aligned} \quad (13)$$

in which $\mathbf{x}_{(0)}^{\mathrm{a}}$ is equal to $\mathbf{x}_0^{\mathrm{b}}$. Based on the above approximation, the minimizer of the cost function (4) is

$$\begin{aligned} \mathbf{x}_{(n+1)}^{\mathrm{a}} = & \mathbf{x}_{(n)}^{\mathrm{a}} + \left[\left[\mathbf{P}_{(n)}^{\mathrm{a}}\right]^{-1} + \mathbf{M}_n^{\mathrm{T}}\mathbf{H}_n^{\mathrm{T}}\mathbf{R}_n^{-1}\mathbf{H}_n\mathbf{M}_n\right]^{-1} \\ & \times \mathbf{M}_n^{\mathrm{T}}\mathbf{H}_n^{\mathrm{T}}\mathbf{R}_n^{-1}\left[\mathbf{y}_n^{\mathrm{obs}} - H_n\left(M_n\left(\mathbf{x}_{(n)}^{\mathrm{a}}\right)\right)\right]. \end{aligned} \quad (14)$$

The analysis $\mathbf{x}_{(n+1)}^{\mathrm{a}}$ assimilates retrospectively an observation set $\mathbf{y}_n^{\mathrm{obs}}$ at a future time t_n into the prior analysis $\mathbf{x}_{(n)}^{\mathrm{a}}$, which is still at time t_0. With reference to the derivation of $\mathbf{P}_{(1)}^{\mathrm{a}}$, we know that the error covariance of the analysis $\mathbf{x}_{(n+1)}^{\mathrm{a}}$ is

$$\mathbf{P}_{(n+1)}^{\mathrm{a}} = \left[\left[\mathbf{P}_{(n)}^{\mathrm{a}}\right]^{-1} + \mathbf{M}_n^{\mathrm{T}}\mathbf{H}_n^{\mathrm{T}}\mathbf{R}_n^{-1}\mathbf{H}_n\mathbf{M}_n\right]^{-1}. \quad (15)$$

We define ROI by eqs. (14) and (15). Note that tangent linear and adjoint models are found in the both equations. The equivalence between ROI and QSVA is analogous to the equivalence between the extended Kalman filter and 4D-Var (Lorenc, 1986).

2.3. Comparison of ROI with 4D-Var

As the time interval between the analysis time and the observation set to be assimilated increases, the non-linearity of the forward model operator $M_n(\mathbf{x})$ also generally increases. As the non-linearity of $M_n(\mathbf{x})$ becomes greater, the Euclidean norm of perturbation, in which a tangent linear approximation of $M_n(\mathbf{x})$ around any state is allowed, becomes smaller. To the extent that the model correctly represents the true system, the global minimizer of the cost function (1) is likely to be found in the vicinity of the true state. ROI forces $\mathbf{x}^{\mathrm{a}}_{(n)}$ to approach the global minimizer as the iteration number n increases. If the analysis correction of ROI is accurate enough to compensate for the increased nonlinearity of $M_n(\mathbf{x})$, we can expect the assumption (13) to be valid. At this stage, the cost function (1) is approximated by

$$\begin{aligned} J_N(\mathbf{x}_0) &= \left[\mathbf{x}_0 - \mathbf{x}^{\mathrm{b}}_0\right]^{\mathrm{T}} \mathbf{B}^{-1} \left[\mathbf{x}_0 - \mathbf{x}^{\mathrm{b}}_0\right] \\ &+ \sum_{n=0}^{N} \left[\mathbf{y}^{\mathrm{obs}}_n - H_n\left(M_n\left(\mathbf{x}^{\mathrm{a}}_{(n)}\right)\right) - \mathbf{H}_n\mathbf{M}_n\left[\mathbf{x}_0 - \mathbf{x}^{\mathrm{a}}_{(n)}\right]\right] \mathbf{R}^{-1}_n \\ &\times \left[\mathbf{y}^{\mathrm{obs}}_n - H_n\left(M_n\left(\mathbf{x}^{\mathrm{a}}_{(n)}\right)\right) - \mathbf{H}_n\mathbf{M}_n\left[\mathbf{x}_0 - \mathbf{x}^{\mathrm{a}}_{(n)}\right]\right], \end{aligned} \tag{16}$$

around the global minimizer. We call the cost function (16) the relaxed cost function. In Appendix B, we prove that the final analysis $\mathbf{x}^{\mathrm{a}}_{(N+1)}$ of ROI is the minimizer of the quadratic cost function (16). This means that ROI analysis provides a global minimizer of (1) if (13) is valid.

In general, 4D-Var chooses the background state $\mathbf{x}^{\mathrm{a}}_{(0)}$ as the starting state for the iteration procedure. If the cost function (1) has multiple minima, the minimizer that is found by the 4D-Var method may be a local minimizer near the starting state. In 4D-Var, if the tangent linear approximation,

$$\begin{aligned} H_n\left(M_n\left(\mathbf{x}_0\right)\right) &\approx H_n\left(M_n\left(\mathbf{x}^{\mathrm{a}}_{(0)}\right)\right) \\ &+ \mathbf{H}_n\mathbf{M}_n\left[\mathbf{x}_0 - \mathbf{x}^{\mathrm{a}}_{(0)}\right] \quad \text{for } n = 0, \ldots, N, \end{aligned} \tag{17}$$

is valid around the global minimizer, the local minimizer is equal to the global minimizer. The validity of (17) is more difficult to guarantee than that of the eq. (13). If the involved dynamics is linear and multiple minima do not exist, ROI would produce the same result as the 4D-Var analysis. When 4D-Var fails to find the global minimum, we can still expect that the ROI will find the global minimum of the cost function. In the next section, we will show how to additionally obviate the need for an adjoint model in implementing ROI.

3. Strategies for implementing ROI

By using a variant of the Sherman–Woodbury–Morrison formula (Kalnay, 2003), the ROI formulation may be rewritten. The modified equation set is as follows:

$$\begin{aligned} \mathbf{x}^{\mathrm{a}}_{(n+1)} &= \mathbf{x}^{\mathrm{a}}_{(n)} + \mathbf{P}^{\mathrm{a}}_{(n)}\mathbf{M}^{\mathrm{T}}_n\mathbf{H}^{\mathrm{T}}_n\left[\mathbf{H}_n\mathbf{M}_n\mathbf{P}^{\mathrm{a}}_{(n)}\mathbf{M}^{\mathrm{T}}_n\mathbf{H}^{\mathrm{T}}_n + \mathbf{R}_n\right]^{-1} \\ &\times \left[\mathbf{y}^{\mathrm{obs}}_n - H_n\left(M_n\left(\mathbf{x}^{\mathrm{a}}_{(n)}\right)\right)\right], \end{aligned} \tag{18}$$

$$\mathbf{P}^{\mathrm{a}}_{(n+1)} = \mathbf{P}^{\mathrm{a}}_{(n)} - \mathbf{P}^{\mathrm{a}}_{(n)}\mathbf{M}^{\mathrm{T}}_n\mathbf{H}^{\mathrm{T}}_n[\mathbf{H}_n\mathbf{M}_n\mathbf{P}^{\mathrm{a}}_{(n)}\mathbf{M}^{\mathrm{T}}_n\mathbf{H}^{\mathrm{T}}_n + \mathbf{R}_n]^{-1}\mathbf{H}_n\mathbf{M}_n\mathbf{P}^{\mathrm{a}}_{(n)}. \tag{19}$$

The matrix products $\mathbf{H}_n\mathbf{M}_n\mathbf{P}^{\mathrm{a}}_{(n)}$ and $\mathbf{P}^{\mathrm{a}}_{(n)}\mathbf{M}^{\mathrm{T}}_n\mathbf{H}^{\mathrm{T}}_n$ include the tangent linear ($\mathbf{M}_n$) and adjoint ($\mathbf{M}^{\mathrm{T}}_n$) models. However, by applying the perturbation method of Errico and Raeder (1999) to the matrix multiplications, $\mathbf{H}_n\mathbf{M}_n\mathbf{P}^{\mathrm{a}}_{(n)}$ and $\mathbf{P}^{\mathrm{a}}_{(n)}\mathbf{M}^{\mathrm{T}}_n\mathbf{H}^{\mathrm{T}}_n$, we can obviate the need for tangent linear and adjoint models in implementing ROI.

Suppose that a state vector $\mathbf{x}$ is modified by the addition of a deviation $\delta\mathbf{x}$ from a reference state $\mathbf{x}^{\mathrm{r}}$; additionally, a nonlinear and differentiable function $f(\mathbf{x})$ is operating on $\mathbf{x}$. If the Euclidean norm of $\delta\mathbf{x}$ is sufficiently small to validate the tangent linear approximation, we can approximate

$$\left.\frac{\partial f}{\partial \mathbf{x}}\right|_{\mathbf{x}=\mathbf{x}^{\mathrm{r}}} \delta\mathbf{x} \approx f(\mathbf{x}^{\mathrm{r}} + \delta\mathbf{x}) - f(\mathbf{x}^{\mathrm{r}}). \tag{20}$$

Applying (20) to calculation of the matrix multiplications, $\mathbf{H}_n\mathbf{M}_n\mathbf{P}^{\mathrm{a}}_{(n)}$ and $\mathbf{P}^{\mathrm{a}}_{(n)}\mathbf{M}^{\mathrm{T}}_n\mathbf{H}^{\mathrm{T}}_n$, however, the result may have errors originating from higher-order terms.

By adopting scale factors, Errico and Raeder (1999) proposed a perturbation method that calculates the multiplication of the Jacobian $.\frac{\partial f}{\partial \mathbf{x}}|_{\mathbf{x}=\mathbf{x}^r}$ and the deviation $\delta\mathbf{x}$ irrespective of the Euclidean norm of $\delta\mathbf{x}$:

$$\left.\frac{\partial f}{\partial \mathbf{x}}\right|_{\mathbf{x}=\mathbf{x}^r} \delta\mathbf{x} \approx \frac{f(\mathbf{x}^{\mathrm{r}} + s\delta\mathbf{x}) - f(\mathbf{x}^{\mathrm{r}})}{s}, \tag{21}$$

where s is much smaller than 1. Errico and Raeder (1999) used (21) to obtain the TLM of the Mesoscale Adjoint Modeling System version 2.

When ROI is implemented with the perturbation method and the state dimension m is large, it is computationally intensive to evolve the background error covariance. It is also a heavy computational burden to calculate the inverse matrix $[\mathbf{H}_n\mathbf{M}_n\mathbf{P}^{\mathrm{a}}_{(n)}\mathbf{M}^{\mathrm{T}}_n\mathbf{H}^{\mathrm{T}}_n + \mathbf{R}_n]^{-1}$ in eqs. (18) and (19). These computational cost problems also hinder the implementation of the Kalman filter or Kalman smoother (Kalnay, 2003).

However, an efficient algorithm can be devised by assuming accuracy-saturation. In the efficient algorithm, we neglect all errors that are smaller in magnitude than a pre-defined value, called the error tolerance. Since eq. (19) implies that the error variance of each variable in the analysis state vector decreases after an individual ROI analysis step, the number of accuracy-saturated variables cannot decrease as the ROI analysis progresses. For $l \geq k$, we create a $k \times l$ transform matrix $\mathbf{S}_{(n)}$ that filters the (l–k) components of the l-dimensional vector $\mathbf{s}^{\mathrm{a}}_{(n)}$, of which the error variance is smaller than the squared error tolerance. Here, $\mathbf{s}^{\mathrm{a}}_{(0)}$ is equal to $\mathbf{x}^{\mathrm{b}}_0$. By using the transform matrix $\mathbf{S}_{(n)}$, we transform $\mathbf{s}^{\mathrm{a}}_{(n)}$ into a state vector $\mathbf{s}^{\mathrm{b}}_{(n)}$ in k-dimensional analysis subspace,

$$\mathbf{s}^{\mathrm{b}}_{(n)} = \mathbf{s}_{(n)}\mathbf{s}^{\mathrm{a}}_{(n)}. \tag{21}$$

We can rewrite (14) for the analysis subspace as

$$\begin{aligned} \mathbf{s}^{\mathrm{a}}_{(n+1)} &= \mathbf{s}^{\mathrm{b}}_{(n)} + \left[\left[\mathbf{S}_{(n)}\mathbf{P}^{\mathrm{s}}_{(n)}\mathbf{S}^{\mathrm{T}}_{(n)}\right]^{-1} + [\mathbf{H}_n\mathbf{M}_n\mathbf{T}_{(n)}]^{\mathrm{T}}\mathbf{R}^{-1}_n\mathbf{H}_n\mathbf{M}_n\mathbf{T}_{(n)}\right]^{-1} \\ &\times \mathbf{T}^{\mathrm{T}}_{(n)}\mathbf{M}^{\mathrm{T}}_n\mathbf{H}^{\mathrm{T}}_n\mathbf{R}^{-1}_n\left[\mathbf{y}^{\mathrm{obs}}_n - H^s_n\left(\mathbf{s}_{(n)}\right)\right], \end{aligned} \tag{22}$$

where $\mathbf{s}^{\mathrm{a}}_{(n+1)}$ has the same dimension (k) as $\mathbf{s}^{\mathrm{b}}_{(n)}$. When $\mathbf{S}_{(-1)}$ and $\mathbf{n}_{(n)} = \sum_{i=0}^{n}\mathbf{T}^{\mathrm{T}}_{(i-1)}[\mathbf{s}^{\mathrm{a}}_{(i)} - \mathbf{S}^{\mathrm{T}}_{(i)}\mathbf{s}^{\mathrm{b}}_{(i)}]$ is an $m \times m$ identity matrix, $\mathbf{T}_{(n)} = \prod_{i=n}^{0}\mathbf{S}_{(i)}$ and $H^{\mathrm{s}}_n(\mathbf{s}_{(n)}) = H_n(M_n(\mathbf{T}^{\mathrm{T}}_{(n)}\mathbf{s}_{(n)} + \mathbf{n}_{(n)}))$. The corresponding error covariance $\mathbf{P}^{s}_{(n+1)}$ is

$$\mathbf{P}^{s}_{(n+1)} = \left[\left[\mathbf{P}^{s}_{(n)}\right]^{-1} + [\mathbf{H}_n\mathbf{M}_n\mathbf{T}_{(n)}]^{\mathrm{T}}\mathbf{R}_n^{-1}\mathbf{H}_n\mathbf{M}_n\mathbf{T}_{(n)}\right]^{-1}. \tag{23}$$

The ROI analysis in the full dimensional space then becomes:

$$\mathbf{x}^{a}_{(n+1)} = \mathbf{T}^{\mathrm{T}}_{(n)}\mathbf{s}^{a}_{(n+1)} + \mathbf{T}^{\mathrm{T}}_{(n-1)}\mathbf{n}_{(n)}. \tag{24}$$

Eqs. (22)–(24) consist of the reduced-rank formulation of ROI. Applying the perturbation method represented by the eq. (21) to calculation of the matrix multiplication $\mathbf{H}_n\mathbf{M}_n\mathbf{T}_{(n)}$, we obtain

$$\mathbf{H}_n\mathbf{M}_n\mathbf{t}^{r}_{(n)} = \frac{1}{\alpha_r}\left[H_n\left(M_n\left(\mathbf{x}^{a}_{(n)} + \alpha_r\mathbf{t}^{r}_{(n)}\right)\right) - H_n\left(M_n\left(\mathbf{x}^{a}_{(n)}\right)\right)\right] \tag{25}$$

Here, the rth column vector $\mathbf{t}^{r}_{(n)}$ of the matrix $\mathbf{T}_{(n)}$ is scaled by the factor α_r for application of the perturbation method, and $r = 1, 2, \ldots k$.

4. Application of ROI to simple models

4.1. Numerical experiments to examine the capability of ROI in dealing with multiple minima

In this section, we confirm that the final analysis of ROI agrees with the 4D-Var minimizer by showing that the cost function (1) is successfully relaxed into the quadratic cost function (16). The dynamical model used for our experiment is the three-variable Lorenz model, defined as

$$\frac{\mathrm{d}X}{\mathrm{d}t} = \sigma X + \sigma Y, \tag{26a}$$

$$\frac{\mathrm{d}Y}{\mathrm{d}t} = XZ + rX - Y, \tag{26b}$$

$$\frac{\mathrm{d}Z}{\mathrm{d}t} = XY - bZ, \tag{26c}$$

where the parameters σ and b are the Prandtl number and a wavenumber-dependent dissipation coefficient, respectively. The parameter r is proportional to the Rayleigh number (Lorenz, 1963). In our experiment, these parameters are set to be 10, 8/3 and 28, respectively, and such a parameter set drives the system into a chaotic regime.

To examine the performance of ROI and 4D-Var, we form a background $\mathbf{x}^{b}_{0}$ by adding normally distributed random numbers with zero mean and one standard deviation to the component X^{t}_{0} of the initial true state (X^{t}_{0}, Y^{t}_{0}, Z^{t}_{0}) = (–6.177, –10.144, 15.607). Nine sets of observations, (X^{0}_{n}, Y^{0}_{n}, Z^{0}_{n}), made from times t_0 to t_8 are generated, and are normally distributed about the true state with zero means and uncorrelated error variances of 0.25. We determine the true states in time by integrating (26) from (X^{t}_{0}, Y^{t}_{0}, Z^{t}_{0}), using a third-order Runge–Kutta scheme with a dimensionless time step of 0.01. We test two dimensionless observation time intervals, 0.25 and 0.50. The cost function (1) has a unique minimum when the observation time interval is 0.25. When the observation time interval is 0.50, however, the cost function has multiple minima. We carry out an experiment with an observation time interval of 0.70 to show the limitations of ROI in overcoming the multiple minima problem. For the minimization process of 4D-Var, we use the steepest descent method since, in this experiment, we will focus only on the accuracy of 4D-Var analysis, not on its efficiency.

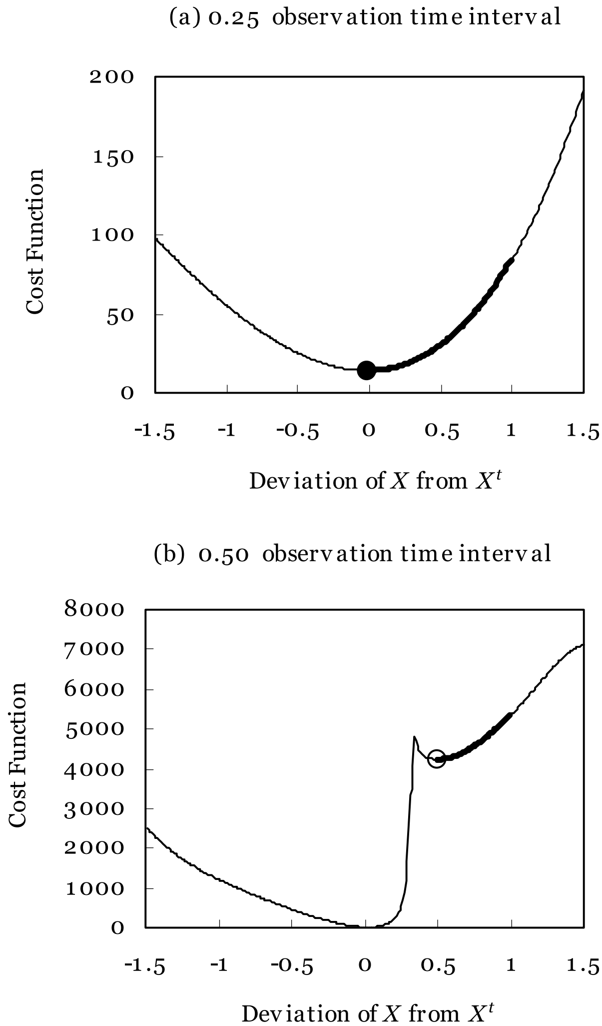

Fig. 1. The cost function of the variable X for the (a) 0.25 and (b) 0.50 observation time intervals in the Lorenz three-variable experiment. The thick portions of the curves denote the course of the minimization process. In (a), the minimizer obtained by 4D-Var is equal to its global minimizer denoted by a solid dot, but in (b), the minimization process is trapped in the local minimum, as indicated by an empty dot.

In Fig. 1a, we plot the cost function (1) for $N = 8$ and the 0.25 observation time interval. It has a unique minimum, and thus, the 4D-Var analysis denoted by a black dot is equal to the global minimizer. When the observation time interval is 0.50, there are multiple minima (Fig. 1b). As discussed in Section 2, 4D-Var does not produce the global minimizer in this case.

Table 1 shows the previous analyses of ROI from $\mathbf{x}^{a}_{(0)}$ to $\mathbf{x}^{a}_{(8)}$ and the final analysis $\mathbf{x}^{a}_{(9)}$. By using the previous analyses to

Table 1. Deviations of the ROI analysis states, obtained by assimilating the observation sets successively from the minimizer X^m = 0.016 of the cost function at the 0.50 observation time interval in the Lorenz three-variable model experiment

Analysis State	Deviation from X^m
$X^a_{(0)}$	0.984
$X^a_{(1)}$	0.584
$X^a_{(2)}$	0.726
$X^a_{(3)}$	– 0.023
$X^a_{(4)}$	– 0.011
$X^a_{(5)}$	0.007
$X^a_{(6)}$	0.002
$X^a_{(7)}$	0.003
$X^a_{(8)}$	0.009
$X^a_{(9)}$	0.001

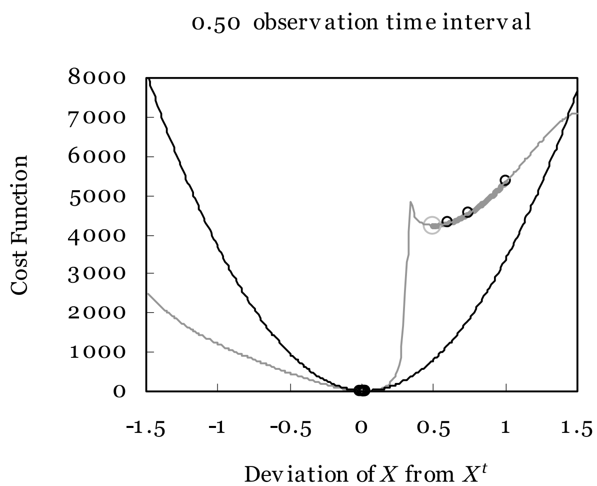

Fig. 2. The relaxed quadratic cost function (black parabola) in the case of Fig. 1(b) with the original cost function (grey curve). The ROI analyses are marked by black empty dots, and the final analysis is at the coordinate (0.02, 13.229). The ROI analyses near the global minimum overlap each other. The bold part of the grey curve shows the minimization procedure of 4D-Var, and the 4D-Var analysis (grey empty dot) is trapped at the local minimum (0.5, 4233.2).

linearize the model operators, we make a quadratic cost function (17) corresponding to the original cost function. Figure 2 demonstrates that the quadratic cost function has a unique minimum almost equal to the global minimum, and the final analysis $\mathbf{x}^a_{(9)}$ of ROI is very close to the global minimizer. Moreover, we observe that the switch to the global minimum state happens after three iterations.

In addition, we test another case with a longer observation time interval of 0.70 (Fig. 3). The 4D-Var minimization procedure is trapped in a local minimum near the background. The ROI final analysis is closer to the global minimum than the 4D-Var analysis though it does not find the global minimum. ROI can extend the effective length of analysis window, but that extension is limited as revealed in our experiment.

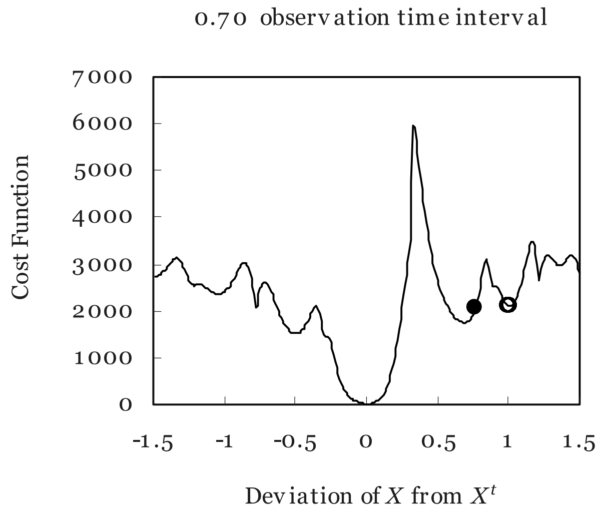

Fig. 3. The cost function of variable *X* for an observation time interval of 0.70 in the Lorenz three-variable model experiment. The 4D-Var minimization procedure was trapped in a local minimum near the background, marked by an empty circle. The solid dot shows an ROI final analysis that is closer to the global minimizer than that of 4D-Var analysis.

4.2. Feasibility of the reduced-rank formulation of ROI

In this subsection, we compare ROI using a reduced-rank formulation with 4D-VAR. The degrees of freedom of the Lorenz 3-variable model are too small to show the effectiveness of the reduced-rank formulation. Therefore, we will use the Lorenz-96 model, which has 40 variables (Lorenz, 1996). The model has *J* grid points spaced equally along a certain latitude circle. The model's equations, which are integrated numerically by a fourth-order Runge–Kutta scheme, are

$$d\mathbf{x}_j/dt = (\mathbf{x}_{j+1} - \mathbf{x}_{j-2})\mathbf{x}_{j-1} - \mathbf{x}_j + F, \tag{27}$$

where $j = 1, \ldots, J$ denotes the longitudinal coordinate. Following Fertig et al. (2007), we set *J* equal to 40, the external forcing *F* to 8 and the time step *t* to 0.05, which roughly corresponds to 6 h in a global weather model (Lorenz and Emmanuel, 1998).

We integrate the model (27) for 5 yr starting with an arbitrary initial condition and assume the resulting state to be the truth. We calculate the background error covariance matrix **B** using 120 samples of states obtained from 30-day integrations stemming from the true state. By adding uncorrelated random noise with a Gaussian distribution with zero mean and the error covariance **B** to the true state, we produce a background state. Twenty observation positions are randomly selected once and used for all experiments, and the observations are made by adding uncorrelated random noise with a Gaussian distribution, with zero mean and the variance of one, to the true state at each

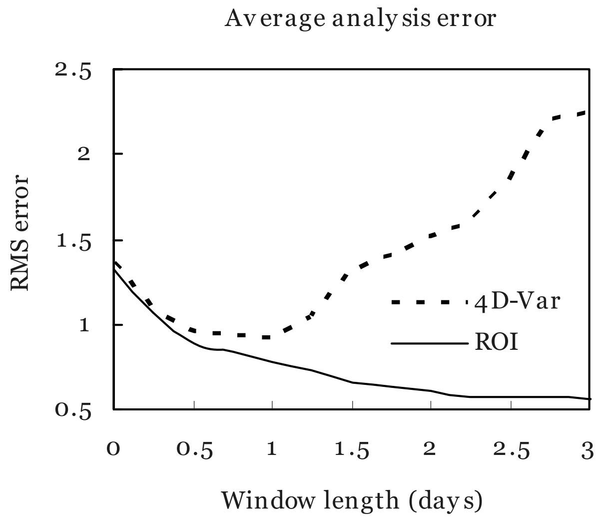

Fig. 4. The average analysis error as a function of the analysis window for 4D-Var (dashed) and ROI (solid) in the Lorenz 40-variable model experiment. Here, the ROI error tolerance is set to zero. The error is defined as the root mean squared (rms) difference between the true state and the corresponding analysis state. The values of analysis errors are obtained by averaging them over 30 realizations.

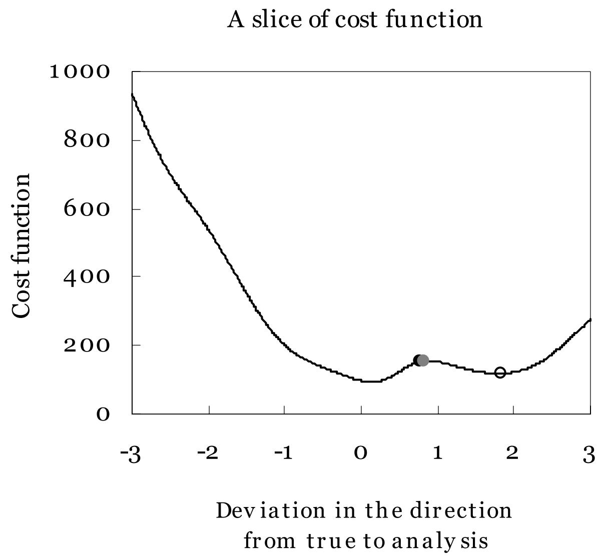

Fig. 5. A slice of the cost function at an analysis window of 2 d in the case of Fig. 4. The cost function has been sliced along with the 4D-Var analysis from the true state. The function value of the global minimum is 0.936, and the local minimum has a value of 1.187. The 4D-Var analysis is shown by an empty circle. The optimal ROI analysis and suboptimal analysis are denoted by black and grey dots, respectively.

observation time. The same true and background states and observations are used for ROI and 4D-Var. For the minimization process of 4D-Var, we use a Broyden–Fletcher–Goldfarb–Shanno (BFGS) algorithm (which is more efficient than the steepest descent method used for the Lorenz three-variable experiments), since we want to compare the efficiency of ROI with that of 4D-Var (Press et al., 1992). According to the results of several tests (not shown), we conclude that a cost function gradient of 0.01 is enough to guarantee the convergence of the minimization algorithm of 4D-Var, and thus set the tolerance of the gradient to 0.01.

To evaluate the accuracy of the ROI and 4D-Var analyses, we compute the root-mean-squared (rms) difference between the true state and the analysis state and define it as analysis error. Next, the average analysis error is obtained by averaging the analysis errors over 30 realizations. We show the average analysis error as a function of the analysis window in Fig. 4 for 4D-Var (dashed) and ROI (solid). In this case, the ROI error tolerance was set to be zero. We see that the average analysis error of 4D-Var increases for analysis windows longer than 1 d, whereas that of ROI decreases as the analysis window is extended.

The eq. (27) multiplies two time-dependent variables. This nonlinearity in the Lorenz 40-variable model can cause the cost function of 4D-Var to have multiple minima. The accuracy of the 4D-Var analysis does not reach that of ROI for analysis windows longer than 0.5 d. This implies that the minimization procedure stopped after finding a local minimum. To check the existence of multiple minima, we draw a slice of the cost function along a line in the state space to connect the 4D-Var analysis to the true state for an analysis window of 2 d. We also plot ROI analysis results (solid dot) with those of 4D-Var analysis (empty circle) in Fig. 5. As shown in Fig. 5, we find that the global minimum of the cost function is 0.936, and the local minimum is 1.187. The 4D-Var analysis has been trapped in the local minimum. By setting the error tolerance to 1.1, we obtained a suboptimal ROI analysis, which requires 0.17 times as much computation time as the 4D-Var analysis, and it is denoted by a grey dot. The suboptimal ROI analysis like the optimal analysis has escaped the local minimum.

The ROI computing times and analysis errors, which vary with the ROI error tolerance, are divided by those of 4D-Var in the respective analysis windows and are named relative rms error and relative computing time, respectively. We plot the relative rms error and the relative computing time as a function of error tolerance in Fig. 6. As the error tolerance increases in the reduced-rank formulation of ROI, the relative rms error increases, whereas the relative computing time decreases. In other words, computation cost is reduced at the expense of analysis accuracy. As the analysis window increases, the relative rms error tends to decrease, as does the relative computing time. This tendency becomes distinct for analysis windows greater than or equal to 24 h and suggests that the efficiency of the reduced-rank formulation increases as the analysis window expands in time length.

ROI analysis error is plotted against computational cost in Fig. 7 for analysis windows of 12, 24, 36 and 48 h. For the assimilation windows of 12 and 24 h, there are some sections in which relative rms errors exceed one. In this range of the parameters, it seems that the ROI analysis errors due to omission of the accuracy-saturated analysis components are large, whereas the

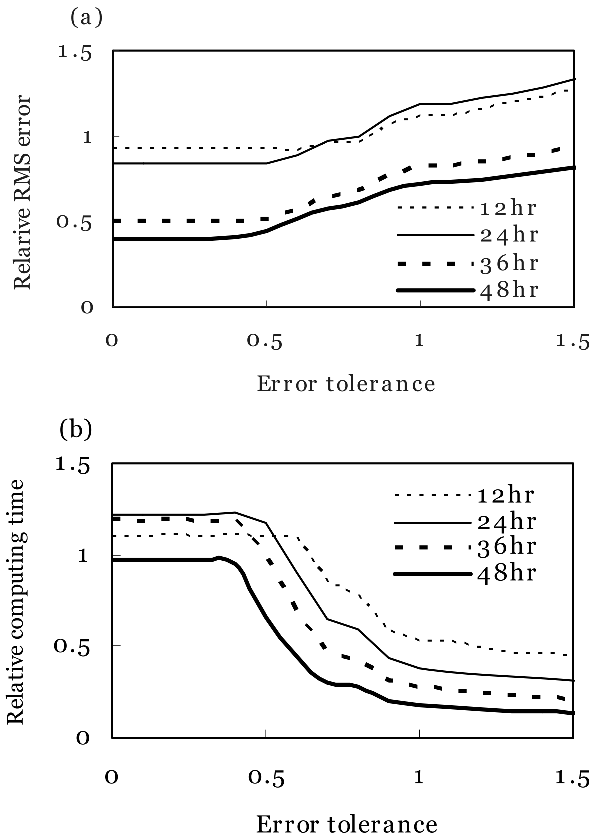

Fig. 6. (a) The relative analysis error and (b) the relative computing time versus the error tolerance for analysis windows of 12 (dashed line), 24 (solid line), 36 (dashed bold line) and 48 h (solid bold line) in the Lorenz 40-variable model experiment. The relative computing times and the relative rms errors of ROI are defined as the values divided by those of 4D-Var for the respective analysis windows.

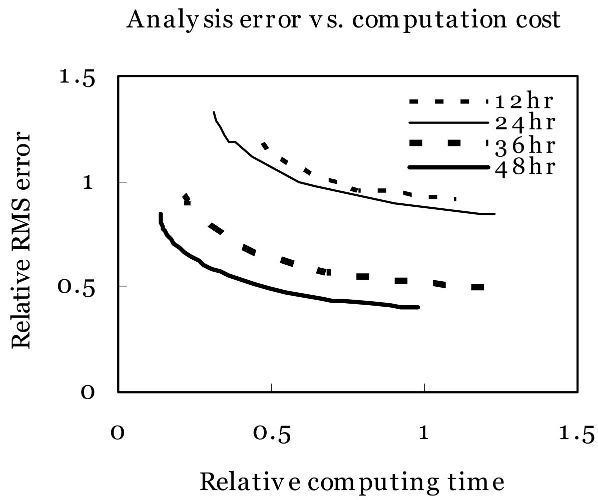

Fig. 7. The relative analysis error versus the relative computational cost for analysis windows of 12, 24, 36 and 48 h in the Lorenz 40-variable model experiment. The computing times and analysis errors of ROI are divided by those of 4D-Var for the respective analysis windows.

errors of the 4D-Var analysis due to the multiple minima problem are relatively small. Nevertheless, the corresponding relative computing times are less than one. For assimilation windows of 36 and 48 h, we obtain the same analysis quality at less cost than that required by 4D-Var in most parameter ranges. With the same computation costs, ROI produced a more accurate analysis than 4D-Var. Therefore in these cases, the ROI analysis error due to the reduced-rank formulation was small enough to overcome the error due to the multiple minima problem.

Note that the numerical model used for our experiment has 40 variables, whereas realistic models typically have over a million degrees of freedom. When ROI is applied to a realistic model, the number of model integrations necessary to evolve the transformation matrix $\mathbf{T}_{(n)}$ is huge. The dimension of the matrix to be inverted in the ROI analysis equation is equal to the number of model integrations. The results shown in Fig. 7 therefore do not guarantee that ROI is more efficient than 4D-Var in realistic applications. It does show, however, that we can reduce the huge computational costs of implementing ROI by exploiting the reduced-rank formulation within a range of acceptable error.

5. Conclusions

We derived the ROI algorithm from the QSVA algorithm proposed by Pires et al. (1996). The assumption that 4D-Var produces the same analysis as the global minimizer, is more difficult to justify than the tangent linear assumption, which is required for the optimality of ROI. When 4D-Var fails to find the global minimum, we can still expect that ROI will find the global minimum of the cost function. We confirmed our hypothesis with a numerical experiment using the three-variable Lorenz model. The ability of ROI to overcome the multiple minima problem is, however, valid for a limited range of time interval between the observations, as shown in Fig. 3.

By adopting the perturbation method by Errico and Raeder (1999), we can implement ROI without using a tangent linear model and the corresponding adjoint model. In addition, the accuracy-saturation property of ROI is exploited to devise a reduced-rank formulation to curtail the high computational cost. From Lorenz 40-variable model experiments, we confirmed that the reduced-rank formulation may improve the efficiency of ROI. The efficiency becomes high as the analysis window increases.

Realistic models typically have over a million degrees of freedom. When ROI is applied to a realistic model, the number of model integrations necessary to evolve the transformation matrix is huge. The dimension of the matrix to be inverted in the ROI analysis equation is equal to the number of model integrations. We will evaluate the effect of the reduced-rank formulation on the reduction of the huge computational costs of implementing ROI in future study.

6. Acknowledgments

This research was supported by the Korea Foundation for International Cooperation of Science & Technology (KICOS) through a grant provided by the Korean Ministry of Education, Science & Technology (MEST) in 2008 (No. K2 0607010001–08A050100110) and the Global Project Partnership for the year of 2008. The first author acknowledges financial support from the Brain Korea 21 Project and the Seoul Science Fellowship. We especially thank Baek-Min Kim for invaluable comments, which clarified the concept of the proposed technique, and Lisa Neef for her thoughtful and delicate review.

Appendix A: The derivation of the analysis error covariance $\mathbf{P}^{\mathbf{a}}_{(\mathbf{1})}$

When $H_0(\mathbf{x}_0^{\mathrm{b}}) - H_0(\mathbf{x}_0^{\mathrm{t}}) \approx \mathbf{H}_0[\mathbf{x}_0^{\mathrm{b}} - \mathbf{x}_0^{\mathrm{t}}]$ and $\mathbf{y}_0^{\mathrm{t}} = H_0(\mathbf{x}_0^{\mathrm{t}})$, with the overbar (-) denoting the expectation of a random variable, we can manipulate the eq. (7) to obtain the corresponding error covariance $\mathbf{P}^{\mathrm{a}}_{(1)}$ as follows:

$$
\begin{aligned}
&\overline{\left[\mathbf{x}^{\mathrm{a}}_{(1)} - \mathbf{x}^{\mathrm{t}}_0\right]\left[\mathbf{x}^{-}_{(1)} - \mathbf{x}^{\mathrm{t}}_0\right]^{\mathrm{T}}} \\
&\quad = \overline{\left[\mathbf{x}_0^{\mathrm{b}} - \mathbf{x}_0^{\mathrm{t}} + \left[\mathbf{B}^{-1} + \mathbf{H}_0^{\mathrm{T}}\mathbf{R}_0^{-1}\mathbf{H}_0\right]^{-1}\mathbf{H}_0^{\mathrm{T}}\mathbf{R}_0^{-1}\left[\mathbf{y}_0^{\mathrm{obs}} - \mathbf{y}_0^{\mathrm{t}} + H_0\left(\mathbf{x}_0^{\mathrm{t}}\right) - H_0\left(\mathbf{x}_0^{\mathrm{b}}\right)\right]\right]} \\
&\quad\ \ \overline{\left[\mathbf{x}_0^{\mathrm{b}} - \mathbf{x}_0^{\mathrm{t}} + \left[\mathbf{B}^{-1} + \mathbf{H}_0^{\mathrm{T}}\mathbf{R}_0^{-1}\mathbf{H}_0\right]^{-1}\mathbf{H}_0^{\mathrm{T}}\mathbf{R}_0^{-1}\left[\mathbf{y}_0^{\mathrm{obs}} - \mathbf{y}_0^{\mathrm{t}} + H_0\left(\mathbf{x}_0^{\mathrm{t}}\right) - H_0\left(\mathbf{x}_0^{\mathrm{b}}\right)\right]\right]^{\mathrm{T}}} \\
&\overline{\left[\mathbf{x}^{\mathrm{a}}_{(1)} - \mathbf{x}^{\mathrm{t}}_0\right]\left[\mathbf{x}^{\mathrm{a}}_{(1)} - \mathbf{x}^{\mathrm{t}}_0\right]^{\mathrm{T}}} \\
&\quad = \overline{[\mathbf{x}_0^{\mathrm{b}} - \mathbf{x}_0^{\mathrm{t}}][\mathbf{x}_0^{\mathrm{b}} - \mathbf{x}_0^{\mathrm{t}}]^{\mathrm{T}}} + [\mathbf{B}^{-1} + \mathbf{H}_0^{\mathrm{T}}\mathbf{R}_0^{-1}\mathbf{H}_0]^{-1}\mathbf{H}_0^{\mathrm{T}}\mathbf{R}_0^{-1}[\overline{[\mathbf{y}_0^{\mathrm{obs}} - \mathbf{y}_0^{\mathrm{t}}][\mathbf{y}_0^{\mathrm{obs}} - \mathbf{y}_0^{\mathrm{t}}]^{\mathrm{T}}} + \\
&\quad\ \ \overline{[H_0(\mathbf{x}_0^{\mathrm{t}}) - H_0(\mathbf{x}_0^{\mathrm{b}})][H_0(\mathbf{x}_0^{\mathrm{t}}) - H_0(\mathbf{x}_0^{\mathrm{b}})]^{\mathrm{T}}}]\mathbf{R}_0^{-1}\mathbf{H}_0[\mathbf{B}^{-1} + \mathbf{H}_0^{\mathrm{T}}\mathbf{R}_0^{-1}\mathbf{H}_0]^{-1} + \\
&\quad\ \ \overline{[\mathbf{B}^{-1} + \mathbf{H}_0^{\mathrm{T}}\mathbf{R}_0^{-1}\mathbf{H}_0]^{-1}\mathbf{H}_0^{\mathrm{T}}\mathbf{R}_0^{-1}[H_0(\mathbf{x}_0^{\mathrm{t}}) - H_0(\mathbf{x}_0^{\mathrm{b}})][\mathbf{x}_0^{\mathrm{b}} - \mathbf{x}_0^{\mathrm{t}}]^{\mathrm{T}}} + \\
&\quad\ \ \overline{[\mathbf{x}_0^{\mathrm{b}} - \mathbf{x}_0^{\mathrm{t}}][H_0(\mathbf{x}_0^{\mathrm{t}}) - H_0(\mathbf{x}_0^{\mathrm{b}})]^{\mathrm{T}}\mathbf{R}_0^{-1}\mathbf{H}_0[\mathbf{B}^{-1} + \mathbf{H}_0^{\mathrm{T}}\mathbf{R}_0^{-1}\mathbf{H}_0]^{-1}} \\
&\mathbf{P}^{\mathrm{a}}_{(1)} = \mathbf{B} + \left[\mathbf{B}^{-1} + \mathbf{H}_0^{\mathrm{T}}\mathbf{R}_0^{-1}\mathbf{H}_0\right]^{-1}\mathbf{H}_0^{\mathrm{T}}\mathbf{R}_0^{-1}\left[\mathbf{R}_0 + \mathbf{H}_0\mathbf{B}\mathbf{H}_0^{\mathrm{T}}\right]\mathbf{R}_0^{-1}\mathbf{H}_0\left[\mathbf{B}^{-1} + \mathbf{H}_0^{\mathrm{T}}\mathbf{R}_0^{-1}\mathbf{H}_0\right]^{-1} \\
&\qquad - \left[\mathbf{B}^{-1} + \mathbf{H}_0^{\mathrm{T}}\mathbf{R}_0^{-1}\mathbf{H}_0\right]^{-1}\mathbf{H}_0^{\mathrm{T}}\mathbf{R}_0^{-1}\mathbf{H}_0\mathbf{B} - \mathbf{B}\mathbf{H}_0^{\mathrm{T}}\mathbf{R}_0^{-1}\mathbf{H}_0\left[\mathbf{B}^{-1} + \mathbf{H}_0^{\mathrm{T}}\mathbf{R}_0^{-1}\mathbf{H}_0\right]^{-1} \\
&\qquad = \mathbf{B} + \left[\mathbf{B}^{-1} + \mathbf{H}_0^{\mathrm{T}}\mathbf{R}_0^{-1}\mathbf{H}_0\right]^{-1}\mathbf{H}_0^{\mathrm{T}}\mathbf{R}_0^{-1}\mathbf{H}_0\left[\mathbf{B}^{-1} + \mathbf{H}_0^{\mathrm{T}}\mathbf{R}_0^{-1}\mathbf{H}_0\right]^{-1} \\
&\qquad + \left[\mathbf{B}^{-1} + \mathbf{H}_0^{\mathrm{T}}\mathbf{R}_0^{-1}\mathbf{H}_0\right]^{-1}\mathbf{H}_0^{\mathrm{T}}\mathbf{R}_0^{-1}\mathbf{H}_0\mathbf{B}\mathbf{H}_0^{\mathrm{T}}\mathbf{R}_0^{-1}\mathbf{H}_0[\mathbf{B}^{-1} + \mathbf{H}_0^{\mathrm{T}}\mathbf{R}_0^{-1}\mathbf{H}_0]^{-1} \\
&\qquad - \left[\mathbf{B}^{-1} + \mathbf{H}_0^{\mathrm{T}}\mathbf{R}_0^{-1}\mathbf{H}_0\right]^{-1}\mathbf{H}_0^{\mathrm{T}}\mathbf{R}_0^{-1}\mathbf{H}_0\mathbf{B}\left[\mathbf{B}^{-1} + \mathbf{H}_0^{\mathrm{T}}\mathbf{R}_0^{-1}\mathbf{H}_0\right]\left[\mathbf{B}^{-1} + \mathbf{H}_0^{\mathrm{T}}\mathbf{R}_0^{-1}\mathbf{H}_0\right]^{-1} \\
&\qquad - \mathbf{B}\mathbf{H}_0^{\mathrm{T}}\mathbf{R}_0^{-1}\mathbf{H}_0\left[\mathbf{B}^{-1} + \mathbf{H}_0^{\mathrm{T}}\mathbf{R}_0^{-1}\mathbf{H}_0\right]^{-1} \\
&\qquad = \mathbf{B} - \mathbf{B}\mathbf{H}_0^{\mathrm{T}}\mathbf{R}_0^{-1}\mathbf{H}_0\left[\mathbf{B}^{-1} + \mathbf{H}_0^{\mathrm{T}}\mathbf{R}_0^{-1}\mathbf{H}_0\right]^{-1} \\
&\qquad = \mathbf{B}\left[\mathbf{B}^{-1} + \mathbf{H}_0^{\mathrm{T}}\mathbf{R}_0^{-1}\mathbf{H}_0\right]\left[\mathbf{B}^{-1} + \mathbf{H}_0^{\mathrm{T}}\mathbf{R}_0^{-1}\mathbf{H}_0\right]^{-1} \\
&\qquad - \mathbf{B}\mathbf{H}_0^{\mathrm{T}}\mathbf{R}_0^{-1}\mathbf{H}_0\left[\mathbf{B}^{-1} + \mathbf{H}_0^{\mathrm{T}}\mathbf{R}_0^{-1}\mathbf{H}_0\right]^{-1} \\
&\qquad = \left[\mathbf{B}^{-1} + \mathbf{H}_0^{\mathrm{T}}\mathbf{R}_0^{-1}\mathbf{H}_0\right]^{-1}.
\end{aligned}
$$

Appendix B: Equality of the final analysis of ROI to the minimizer of the quadratic cost function

When the final analysis $\mathbf{x}^{\mathrm{a}}_{(N+1)}$ of ROI is substituted into the gradient of eq. (16), the following equation is obtained:

$$
\begin{aligned}
&\nabla J_N\left(\mathbf{x}^{\mathrm{a}}_{(N+1)}\right) = \mathbf{B}^{-1}\left[\mathbf{x}^{\mathrm{a}}_{(N+1)} - \mathbf{x}^{\mathrm{b}}\right] \\
&\quad - \sum_{n=o}^{N}\mathbf{M}_n^{\mathrm{T}}\mathbf{H}_n^{\mathrm{T}}\mathbf{R}_n^{-1}[\mathbf{y}_n^{\mathrm{obs}} - H_n(M_n(\mathbf{x}^{\mathrm{a}}_{(n)})) - \mathbf{H}_n\mathbf{M}_n[\mathbf{x}^{\mathrm{a}}_{(N+1)} - \mathbf{x}^{\mathrm{a}}_{(n)}]].
\end{aligned}
\tag{B.1}
$$

If we manipulate this equation as follows,

$$
\begin{aligned}
&\nabla J_N\left(\mathbf{x}^{\mathrm{a}}_{(N+1)}\right) \\
&\quad = \underbrace{\mathbf{B}^{-1}\left[\mathbf{x}^{\mathrm{a}}_{(N)} - \mathbf{x}^{\mathrm{b}}\right] - \sum_{n=0}^{N-1}\mathbf{M}_n^{\mathrm{T}}\mathbf{H}_n^{\mathrm{T}}\mathbf{R}_n^{-1}\left[\mathbf{y}_n^{\mathrm{obs}} - H_n\left(M_n\left(\mathbf{x}^{\mathrm{a}}_{(n)}\right)\right) - \mathbf{H}_n\mathbf{M}_n\left[\mathbf{x}^{\mathrm{a}}_{(N)} - \mathbf{x}^{\mathrm{a}}_{(n)}\right]\right]}_{\nabla J_{N-1}\left(\mathbf{x}^{a}_{(N)}\right)} \\
&\qquad + \mathbf{B}^{-1}\underline{\left[\mathbf{x}^{\mathrm{a}}_{(N+1)} - \mathbf{x}^{\mathrm{a}}_{(N)}\right]} + \sum_{N=0}^{n-1}\mathbf{M}_n^{\mathrm{T}}\mathbf{H}_n^{\mathrm{T}}\mathbf{R}_n^{-1}\mathbf{H}_n\mathbf{M}_n\underline{\left[\mathbf{x}^{\mathrm{a}}_{(N+1)} - \mathbf{x}^{\mathrm{a}}_{(N)}\right]} \\
&\qquad - \mathbf{M}_N^{\mathrm{T}}\mathbf{H}_N^{\mathrm{T}}\mathbf{R}_N^{-1}\left[\mathbf{y}_N^{0} - H_N\left(M_N(\mathbf{x}^{\mathrm{a}}_{(N)}\right) - \mathbf{H}_N\mathbf{M}_N\underline{\left[\mathbf{x}^{\mathrm{a}}_{(N+1)} - \mathbf{x}^{\mathrm{a}}_{(N)}\right]}\right],
\end{aligned}
\tag{B.2}
$$

we can express $\nabla J_N(\mathbf{x}^{\mathrm{a}}_{(N+1)})$ using $\nabla J_{N-1}(\mathbf{x}^{\mathrm{a}}_{(N)})$. By considering the underlined terms, we have the following relationship:

$$\begin{aligned}\nabla J_N\left(\mathbf{x}^{\mathrm{a}}_{(N+1)}\right) &= \nabla J_{N-1}\left(\mathbf{x}^{\mathrm{a}}_{(N)}\right)\\ &-\mathbf{M}_N^{\mathrm{T}}\mathbf{H}_N^{\mathrm{T}}\mathbf{R}_N^{-1}\left[\mathbf{y}_N^{\mathrm{obs}} - H_N M_N\left(\mathbf{x}^{\mathrm{a}}_{(N)}\right)\right]\\ &+\left[\mathbf{B}^{-1}+\sum_{n=0}^{N}\mathbf{M}_n^{\mathrm{T}}\mathbf{H}_n^{\mathrm{T}}\mathbf{R}_n^{-1}\mathbf{H}_n\mathbf{M}_n\right]\underline{\left[\mathbf{x}^{\mathrm{a}}_{(N+1)}-\mathbf{x}^{\mathrm{a}}_{(N)}\right]}.\end{aligned} \tag{B.3}$$

Because the underlined part of this equation is an analysis correction of the *N*th ROI analysis, we find inductively that the value of $\nabla J_N(\mathbf{x}^{\mathrm{a}}_{(N+1)})$ is equal to zero by considering the eq. (14) for ROI, as outlined in detail in the following equation:

$$\begin{aligned}&\nabla J_N\left(\mathbf{x}^{\mathrm{a}}_{(N+1)}\right)\\ &= \nabla J_{N-1}\left(\mathbf{x}^{\mathrm{a}}_{(N)}\right) - \mathbf{M}_N^{\mathrm{T}}\mathbf{H}_N^{\mathrm{T}}\mathbf{R}_N^{-1}\left[\mathbf{y}_N^{\mathrm{obs}} - H_N M_N\left(\mathbf{x}^{\mathrm{a}}_{(N)}\right)\right]\\ &\quad+\left[\mathbf{B}^{-1}+\sum_{n=0}^{N}\mathbf{M}_n^{\mathrm{T}}\mathbf{H}_n^{\mathrm{T}}\mathbf{R}_n^{-1}\mathbf{H}_n\mathbf{M}_n\right]\\ &\quad\times\left[\mathbf{B}^{-1}+\sum_{n=0}^{N}\mathbf{M}_n^{\mathrm{T}}\mathbf{H}_n^{\mathrm{T}}\mathbf{R}_n^{-1}\mathbf{H}_n\mathbf{M}_n\right]^{-1}\\ &\quad\times\mathbf{M}_N^{\mathrm{T}}\mathbf{H}_N^{\mathrm{T}}\mathbf{R}_N^{-1}\left[\mathbf{y}_N^{\mathrm{obs}} - H_N M_N\left(\mathbf{x}^{\mathrm{a}}_{(N)}\right)\right]\\ &= \nabla J_{N-1}\left(\mathbf{x}^{\mathrm{a}}_{(N)}\right) - \mathbf{M}_N^{\mathrm{T}}\mathbf{H}_N^{\mathrm{T}}\mathbf{R}_N^{-1}\left[\mathbf{y}_N^{\mathrm{obs}} - H_N M_N\left(\mathbf{x}^{\mathrm{a}}_{(N)}\right)\right]\\ &\quad+\mathbf{M}_N^{\mathrm{T}}\mathbf{H}_N^{\mathrm{T}}\mathbf{R}_N^{-1}\left[\mathbf{y}_N^{\mathrm{o}} - H_N M_N\left(\mathbf{x}^{\mathrm{a}}_{(N)}\right)\right]\\ &= \nabla J_{N-1}\left(\mathbf{x}^{\mathrm{a}}_{(N)}\right)\\ &\quad\cdots\\ &= \nabla J_0\left(\mathbf{x}^{\mathrm{a}}_{(1)}\right)\\ &= \mathbf{B}^{-1}\left[\mathbf{x}^{\mathrm{a}}_{(1)}-\mathbf{x}^{\mathrm{b}}\right] - \mathbf{H}_0^{\mathrm{T}}\mathbf{R}_0^{-1}\left[\mathbf{y}_0^{\mathrm{obs}} - H_0\left(\mathbf{x}^{\mathrm{a}}_{(1)}\right) - \mathbf{H}_0\left[\mathbf{x}^{\mathrm{a}}_{(1)}-\mathbf{x}^{\mathrm{b}}\right]\right]\\ &= \left[\mathbf{B}^{-1}+\mathbf{H}_0^{\mathrm{T}}\mathbf{R}_0^{-1}\mathbf{H}_0\right]\left[\mathbf{B}^{-1}+\mathbf{H}_0^{\mathrm{T}}\mathbf{R}_0^{-1}\mathbf{H}_0\right]^{-1}\mathbf{H}_0^{\mathrm{T}}\\ &\quad\mathbf{R}_0^{-1}\left[\mathbf{y}_0^{\mathrm{obs}} - H_0\left(\mathbf{x}^{\mathrm{b}}\right)\right] - \mathbf{H}_0^{\mathrm{T}}\mathbf{R}_0^{-1}\mathbf{H}_0\left[\mathbf{y}_0^{\mathrm{obs}} - H_0\left(\mathbf{x}^{\mathrm{b}}\right)\right]\\ &= 0.\end{aligned} \tag{B.3}$$

This proves that the final analysis $\mathbf{x}^{\mathrm{a}}_{(N+1)}$ of ROI is the minimizer of the quadratic cost function (16).

References

Cohn, S. E., Sivakumaran, N. S. and Todling, R. 1994. A fixed-lag Kalman smoother for retrospective data assimilation. *Mon. Wea. Rev.* **122**, 2838–2867.

Errico, R. M. 2003. The workshop on applications of adjoint models in dynamic meteorology. *Bull. Amer. Meteorol. Soc.* **84**, 795–798.

Errico, R. M. and Raeder, K. D. 1999. An examination of the accuracy of the linearization of a mesoscale model with moist physics. *Q. J. R. Meteorol. Soc.* **125**, 169–195.

Fertig, E. J., Harlim, J. and Hunt, B. R. 2007. A comparative study of 4D-VAR and a 4D Ensemble Kalman Filter: perfect model simulations with Lorenz-96. *Tellus* **59A**, 96–100.

Gérard, É. and Saunders, R. 1999. Four-dimensional variational assimilation of special sensor microwave/imager total column water vapour in the ECMWF model. *Q. J. R. Meteorol. Soc.* **125**, 3077–3101.

Horel, J. and Colman, B. 2005. Real-time and retrospective mesoscale objective analyses. *Bull. Am. Meteorol. Soc.* **86**, 1477–1480.

Janiskova, M., Thépaut, J.-N. and Geleyn, J.-F. 1999. Simplified and regular physical parametrizations for incremental four-dimensional variational assimilation. *Mon. Wea. Rev.* **127,** 26–45.

Kalnay, E. 2003. *Atmospheric Modeling, Data Assimilation and Predictability*. Cambridge University Press, New York.

Le Dimet, F.-X. and Talagrand, O. 1986. Variational algorithms for analysis and assimilation of meteorological observations: theoretical aspects. *Tellus* **38A**, 97–110.

Lorenc, A. C. 1986. Analysis methods for numerical weather prediction. *Q. J. R. Meteorol. Soc.* **112**, 1177–1194.

Lorenc, A. C. 2003. The potential of the ensemble Kalman filter for NWP—a comparison with 4D-VAR. *Q. J. R. Meteorol. Soc.* **129**, 3183–3203.

Lorenz, E. N. 1963. Deterministic nonperiodic flow. *J. Atmos. Sci.* **20**, 130–141.

Lorenz, E. N. 1996. Predictability–a problem partly solved. In: *Proceedings of ECMWF on Predictability*, ECMWF, 4–8 September 1995.

Lorenz, E. N. and Emanuel, K. A. 1998. Optimal sites for supplementary weather observations: simulation with a small model. *J. Atmos. Sci.* **55**, 399–414.

Miller, R. N., Ghil, M. and Gauthiez F. 1994. Advanced data assimilation in strongly nonlinear dynamical systems. *J. Atmos. Sci.* **51**, 1037–1056.

Pires, C., Vautard, R. and Talagrand, O. 1996. On extending the limits of variational assimilation in nonlinear chaotic systems. *Tellus* **48A**, 96–121.

Press, W. H., Flannery, B. P., Teukolsky, S. A. and Vetterling W. V. 1992. *Numerical Recipes in Fortran*. Cambridge University Press, New York.

Rabier, F. and Courtier, P. 1992. Four-dimensional assimilation in the presence of baroclinic instability. *Q. J. R. Meteorol. Soc.* **118**, 649–672.

Rabier, F., Thépaut, J.-N. and Courtier, P. 1998. Extended assimilation and forecast experiments with a four-dimensional variational assimilation system. *Q. J. R. Meteorol. Soc.* **124**, 1861–1887.

Ruggiero, F. H., Michalakes, J., Nehrkorn, T., Modica, G. D. and Zou, X. 2006. Development and tests of a new distributed-memory MM5 adjoint. *J. Atmos. Ocean Sci.* **23**, 424–436.

Sun, J. 2005. Initialization and numerical forecast of a supercell storm observed during STEPS. *Mon. Wea. Rev.* **133**, 793–813.

Swanson, K. L., Vautard, R. and Pires, C. 1998. Four-dimensional variational assimilation and predictability in a quasi-geostrophic model. *Tellus* **50A**, 369–390.

Zhu, J. and Kamachi, M. 2000. The role of time step size in numerical stability of tangent linear models. *Mon. Wea. Rev.* **128,** 1562–1572.